SOIL EROSION CAUSED THE INCREASING HOLOCENE RADIOCARBON RESERVOIR EFFECT OF LAKE KANAS IN THE ALTAI MOUNTAINS

Huihui Cao[ID] • Xiaozhong Huang* • Lixiong Xiang

MOE Key Laboratory of Western China's Environmental System (Ministry of Education), College of Earth and Environmental Sciences, Lanzhou University, Lanzhou 730000, China

ABSTRACT. Radiocarbon (^{14}C) dating of the total organic carbon (TOC) content of lacustrine sediments is always affected by a ^{14}C reservoir effect and the ^{14}C dates are often systematically older than the true ages. However, there are few studies of the temporal changes of the ^{14}C reservoir effect, with reference to the specific influencing factors. We collected TOC samples from the Holocene sediments of Lake Kanas, in the southern Altai Mountains, for AMS ^{14}C dating and compared the results with AMS ^{14}C ages based on terrestrial plant macrofossils from the same depths. The results show that the reservoir ages progressively increased from ~0 to ~2800 yr between ~9700 cal BP and ~530 cal BP. As the lake catchment was glaciated prior to the Holocene, and Holocene soils and peats are the main sources of the TOC in the lake sediments, we argue that soil erosion is the major factor contributing to the progressive increase in the reservoir age. Based on previously reported evidence for increasing moisture in central Asia and glacier advances in the mid-to-late Holocene, we suggest that the intensified soil erosion on the hillslopes was caused by increased precipitation during the mid-to-late Holocene and by anthropogenic forest clearance after 1500 cal BP.

KEYWORDS: ^{14}C reservoir effect, Kanas Lake, lacustrine sediments, radiocarbon dating, soil erosion.

INTRODUCTION

Lake sediments are valuable archives of past environmental and climatic changes, and they offer a means of establishing an accurate chronological framework for sedimentation. Accelerator mass spectrometry (AMS) radiocarbon (^{14}C) dating of organic material is currently the most widely used method of dating lake sediments (Björck and Wohlfarth 2001). A chronological framework for lake sediments can be constructed based on the ^{14}C ages of terrestrial plant macrofossils (e.g., Andree et al. 1986; Huang et al. 2018), or on sedimentary total organic carbon (TOC) (e.g., Watanabe et al. 2010; Zhang et al. 2021). The ^{14}C activity of short-lived terrestrial plants is generally in equilibrium with the atmosphere, and the macrofossil ages can be used to provide accurate depositional ages for specific sedimentary strata, with the prerequisite that a negligible amount of time has passed between the growth of the plant material and its deposition within the lake. Although sedimentary TOC and aquatic plant remains can also be employed for this purpose, they are often affected by old carbon contamination and their ^{14}C dates are typically older than their actual depositional age (e.g., Li et al. 2018). The old carbon usually results from the following factors: disequilibrium in the ^{14}C exchange between water and the atmosphere, which leads to lower ^{14}C concentrations in the lake water (Druffel et al. 1983); the influx of groundwater or surface runoff from watersheds with a limestone substrate, which introduces pre-aged carbon (Olsson 2009); biological utilization of dissolved inorganic carbon (DIC) in the lake water (Kwiecien et al. 2008); an inherited reservoir effect from the introduction of sediments from the watershed (Frueh et al. 2012); and the variable contribution of old terrestrial organic material eroded from catchment soils (Blaauw et al. 2011). The lake ^{14}C reservoir effect varies between different geographical units and over time (e.g., Hou et al. 2012; Mischke et al. 2013; Zhou et al. 2014, 2021; Zhou et al. 2015; Chen et al. 2019; Zhou et al. 2020), and assessing the reservoir effect is a priority in the ^{14}C dating of TOC and aquatic plant remains, to establish an accurate chronological framework for lake sediments.

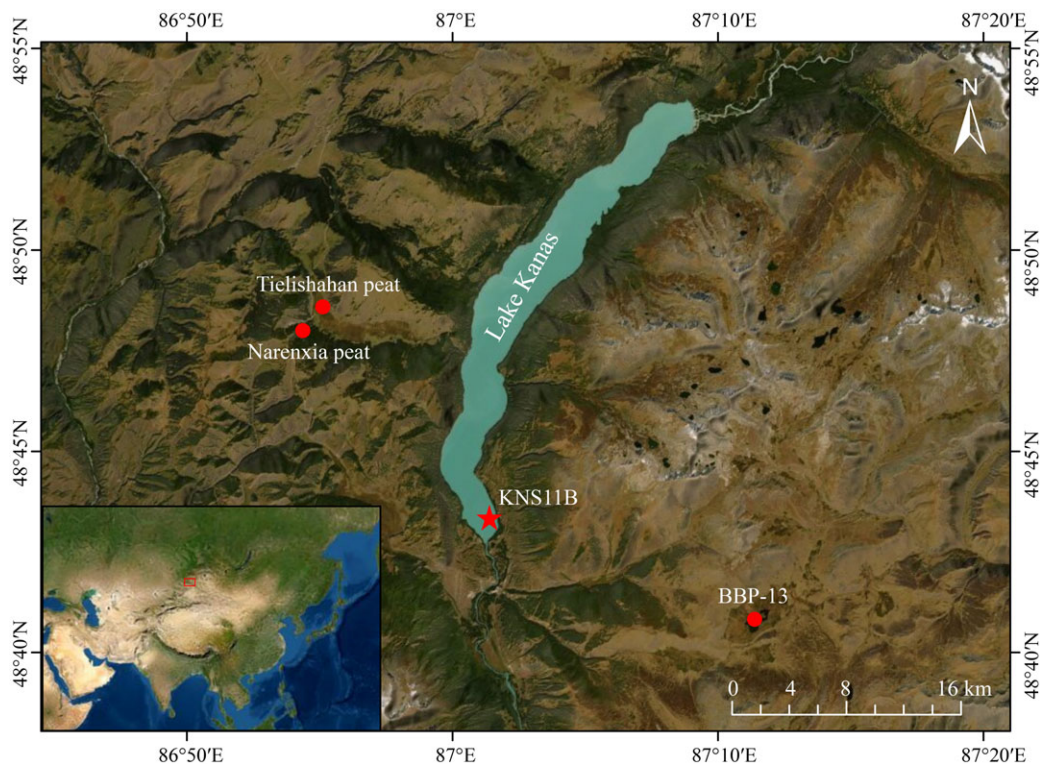*Corresponding author. Email: xzhuang@lzu.edu.cn

Figure 1   Location of Lake Kanas in Asia (inset) and the locations of the sampling site in Lake Kanas and other sites referenced in the text.

Numerous methods have been applied to correct the lake reservoir effect. They include cross-dating approaches with ^{14}C dating and other dating methods (e.g., ^{210}Pb and ^{137}Cs) to evaluate the lake reservoir effect (e.g., Lan et al. 2018; Xu et al. 2021); optical luminescence dating (e.g. Wilkins et al. 2012; An et al. 2018); U-series dating (e.g., Hall et al. 2001; Fan et al. 2014); counting annual laminations (e.g., Tlan et al. 2005; Zhou et al. 2009; Bonk et al. 2015; Zhang et al. 2021); and comparative AMS ^{14}C dating of different materials from the same sedimentary layer to assess the reservoir effect, such as fatty acids (Schroeter et al. 2021), TOC, and terrestrial plant remains (e.g., Huang et al. 2021a). Although AMS ^{14}C dating of terrestrial plant material is a reliable means of quantifying lake sediment ages, terrestrial plant remains are usually scarce in lake sediments in arid central Asia and hence the method is rarely applied.

In the present study, we evaluated temporal changes in the radiocarbon reservoir effect at Lake Kanas by comparing the ^{14}C ages of terrestrial plant remains and sedimentary TOC from the same stratigraphic levels, with the aim of quantifying the effect and determining the processes responsible.

STUDY AREA

Lake Kanas (48.72°N–48.90°N, 87.00°E–87.16°E; altitude of the modern lake surface is 1365 m above sea level) is an open lake in the southern Altai Mountains (Figure 1), at the junction of

westerly airflows and the Siberian high-pressure zone (Aizen et al. 2001). The length of the lake basin is 24 km, and the width is ~2 km; the surface area is nearly 45 km^2 and the average water depth is 120 m (Feng and Ren 1990; Wu et al. 2014). The lake was formed by the damming of a valley by an end moraine that developed during the last glaciation (Xu et al. 2009). Numerous glaciers developed in the northern upper part of the watershed of Lake Kanas during the last glacial period, above 3000 m in elevation, where they reached a total area of ~210 km^2 (Liu et al. 1982). Snow or glacier meltwater and precipitation are the main water sources of Lake Kanas. The bathymetry of the lake basin is steeply sloping and there are no carbonate deposits in the watershed (Wu et al. 2014). The steep-sided lake basin, deep water, and low water temperature limit the growth of aquatic plants, which are nearly absent from the lake basin (Feng and Ren 1990; Lin et al. 2018).

The climate of the region is influenced by the mid-latitude westerlies and polar airmasses, which supply water vapor by precipitation and snowfall in summer and winter. The average annual temperature is ~5.5°C and the precipitation is ~160 mm, based on records from Habahe meteorological station (AD 1958–2014), ~96 km from Lake Kanas (Lin et al. 2018). Due to the topographic effect the precipitation in Lake Kanas is up to 400–700 mm, with a high proportion supplied as winter snowfall (Huang et al. 2018). The snowfall and total precipitation in the high mountains are much higher, reaching ~1000 mm (Feng and Ren 1990; Zhang et al. 2018b).

The vegetation of the Kanas drainage exhibits a pronounced altitudinal zonation, with desert and desert steppe at low elevations (500–1300 m), forest vegetation at intermediate elevations (1300–2300 m), subalpine and alpine meadow at mid-to high elevations (2300–3000 m), and tundra vegetation at high elevations (3000–3500 m) (Xinjiang Comprehensive Survey Team, C. A. o. S., & Institute of Botany, C. A. o. S, 1978). Previous investigations show that widespread peat accumulation occurred in the southern Altai Mountains during 9600–9000 cal BP (Tang et al. 2014; Feng et al. 2017; Zhang et al. 2018a; Wang and Zhang 2019; Xu et al. 2019; Zhang and Elias 2019; Rao et al. 2020). Archaeological surveys show that the number of archaeological sites around Lake Kanas is very limited (Bureau of National Cultural Relics 2012; Huang et al. 2021a), and the impact of human activities on the vegetation may have begun from ~1500 cal BP onwards, based on pollen data (Huang et al. 2018). Additionally, the streams on the hillslopes entering the lake typically have a slight peaty color, while the spring floods, caused by snow meltwater and heavy summer rainfall, may have contributed more old organic matter and humic acids, based on our field observations.

MATERIALS AND METHODS

Sediment core KNS11B (48°43′23″N, 87°01′22″E; length: 244 cm) was collected at a water depth of 19.85 m from the southern part of Kanas Lake using a piston corer (Figure 1). The core was frozen in the field, transported to the laboratory and then sliced into 1-cm intervals. The results of AMS ^{14}C dating of terrestrial plant macrofossils from the core were reported previously (Huang et al. 2018). Nine samples of bulk organic sediments were taken from different depths of the core to determine reservoir ages.

Seven TOC samples of the lake sediments were pretreated using an acid wash procedure. Briefly, 1–2 g samples were weighed and reacted with 0.5 mol/L HCl at 60°C; the acid was replaced daily until the solution became clear, and then washed to neutral and oven-dried

at 60°C. The samples were graphitized using Auto Graphitization Equipment (AGE III) and measured using a compact AMS, Mini Carbon Dating System (MICADAS, IonPlus AG). All the experimental procedures were conducted in the Radiocarbon Laboratory of the MOE Key Laboratory of Western China's Environmental System (Ministry of Education) of Lanzhou University. In addition, two TOC samples were prepared and dated by Beta Analytic (USA). The ^{14}C dates were calibrated to calendar years using the online program OxCal4.4 (Bronk Ramsey 2009) with the IntCal20 curve (Reimer et al. 2020). The results are reported as "cal BP". The Bacon program (version 2.3.9.1) was used for age-depth reconstruction of lake sediments and peat sediments around the lake (Blaauw and Christen 2011), the default settings are selected, with thick is 10, and acc. mean is 20. The IntCal20 database within the program R package was used for ^{14}C date calibration (Reimer et al. 2020).

The acid-washed samples were also used for measurements of their carbon and nitrogen contents, using an Elementar Vario EL Cube at the State Key Laboratory of Applied Organic Chemistry of Lanzhou University. The limit of detection for carbon and nitrogen is 0.0004 mg and 0.0001 mg, respectively, and the analytical error of both elements' contents is less than 0.1%. Additionally, isotopes of organic carbon and nitrogen were measured using an EA-MAT253 at the Third Institute of Oceanography, Ministry of Natural Resources, Xiamen, China. The isotopic values are shown in standard δ-notation in per mil (‰), with respect to Vienna Pee Dee Belemnite (VPDB) carbon and atmospheric nitrogen (N_2). IAEA600 (consensus δ^{13}C: –27.71‰, δ^{15}N:1‰), Acetanilide#1 (consensus δ^{13}C: –26.85‰, δ^{15}N: –4.21‰), and USGS40 (consensus δ^{13}C: –26.39‰, δ^{15}N: –4.52‰) were used as working standards. The analytical error of δ^{13}C and δ^{15}N both not exceeding ±0.2‰.

RESULTS

Details of the ^{14}C dates of the 16 samples from core KNS11B are given in Table 1, including the types of dating material, C/N ratios, and isotopic compositions of the organic materials. The ^{14}C ages of terrestrial plant macrofossils represent their depositional ages, as we assumed, and the ages decrease systematically along the core, from 11,831–11,322 cal BP at 170 cm depth, to 623–501 cal BP at 25 cm depth. The TOC ^{14}C ages are systematically older than the parallel ages obtained by dating plant macrofossils, and the estimated reservoir effect increases along the sequence from the lower to the upper part of the core. The ages of the depths of 135 cm, 117 cm, 101 cm, 88 cm, 73 cm, and 25 cm are 910, 1240, 1110, 1430, 2050, and 2890 ^{14}C years, respectively. The ^{14}C ages of the TOC and charred wood show a reversal at 170-cm depth, which indicates the absence of a radiocarbon reservoir effect and that the residence time of the terrestrial plant material before its incorporation in the sediments was relatively long. The C/N ratios of the sediment samples vary between 9.0 and 14.1, and the δ^{13}C and δ^{15}N values of the TOC vary between –25.7 and –21.5‰ and 3.8 and 7.1‰, respectively.

DISCUSSION

Temporal Variations of the Radiocarbon Reservoir Age in Lake Kanas

The ^{14}C ages of the TOC are systematically older than those of the terrestrial plant remains, indicating an obvious reservoir effect of the TOC-based ^{14}C dates. We simulated the ^{14}C age-depth relationship of the plant residues and TOC to determine the diachronic variations of the radiocarbon reservoir age (Figure 2a). The results show that the reservoir age in Lake Kanas

Table 1 C/N ratios, isotopic compositions, and ^{14}C ages of terrestrial plant macrofossils and TOC from core KNS11B from Lake Kanas (^{14}C ages are calibrated with the IntCal20 curve; Reimer et al. 2020)

Sample ID	Depth (cm)	Material	C (%)	N (%)	C/N ratio	δ^{13}C (‰)	δ^{15}N (‰)	^{14}C lab code	^{14}C age (BP)	Reservoir age (^{14}C years)	Calibrated age of plant remains (BP) (95.4%)
KNS11B-25	25	Plant remains*				–24.6		Beta298010	510 ± 30	2890	623–611 (2.6%)
		TOC	0.885	0.094	9.4	–25.7	5.1	LZU20544	3400 ± 30		555–501 (92.9%)
KNS11B-73	73	Plant remains*				–22.4		Beta298011	1850 ± 30	2050	1830–1702 (94.4%)
		TOC	0.926	0.103	9.0	–25.3	6.1	LZU20545	3900 ± 30		1652–1644 (1.0%)
KNS11B-88	88	Plant remains*				–23.5		Beta298012	2490 ± 30	1430	2724–2463 (94.2%)
		TOC	1.197	0.119	10.1	–25.6	3.8	LZU20546	3920 ± 30		2449–2435 (1.3%)
KNS11B-101	101	Plant remains*				–24.5		Beta298013	3320 ± 40	1110	3680–3670 (1.7%)
		TOC	1.331	0.140	9.5	–25.3	4.0	LZU20547	4430 ± 30		3638–3454 (93.8%)
KNS11B-117	117	Forb stem*				–23.6		Beta298014	4490 ± 40	1240	5305–5030 (90.2%)
		TOC	1.662	0.145	11.5	–25.3	4.1	LZU20548	5730 ± 30		5010–4978 (5.3%)
KNS11B-135	135	Tree twigs*				–27.0		Beta298015	6100 ± 40	910	7158–7102 (15.4%)
		TOC	1.802	0.151	11.9	–25.3	3.9	LZU20549	7010 ± 30		7075–6852 (79.3%)
											6811–6804 (0.8%)
KNS11B-150	150	TOC						Beta336079	7970 ± 40		
KNS11B-160	160	TOC						Beta336080	8590 ± 40		
KNS11B-170	170	Charred wood*				–20.9		Beta298016	10,070 ± 60	N/A	11,831–11,322 (95.4%)
		TOC	0.391	0.028	14.1	–21.5	7.1	LZU20550	9590 ± 40		

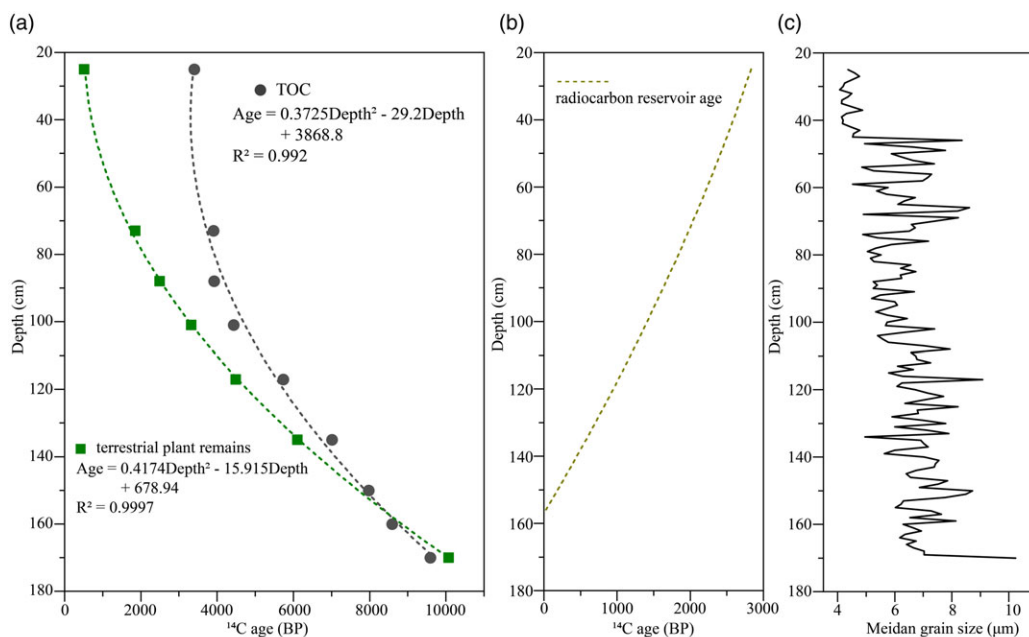*^{14}C age and δ^{13}C of plant remains are from Huang et al. (2018).

Figure 2   (a) Age-depth relationship based on ^{14}C dating of terrestrial plant remains and the TOC content of core KNS11B; (b) depth variation of the radiocarbon reservoir age and (c) median grain size of core KNS11B.

varies from ~0 yr at 156 cm to ~2830 yr at 25 cm below the sediment surface and that it generally increases upwards through the sedimentary sequence (Figure 2b).

Before discussing the reservoir ages it is necessary to assess the reliability of the ^{14}C ages of the seven samples of plant remains, which were published previously (Huang et al. 2018). These plant remains include tree bark, twigs, forb stems, and charred wood, with sizes ranging from several millimeters to centimeters (see photos in the Supporting Information of Huang et al. 2018). The plant remains were in a fresh condition with no evidence of aerobic humification or decay and they clearly demonstrate the characteristics of terrestrial-sourced materials. Lake Kanas is surrounded by numerous trees which shed abundant plant materials, which is confirmed by our investigation of a near-shore sediment core from Lake Kanas that contained terrestrial plant remains (Wang et al. 2017). Additionally, the calculated sedimentation rate (0.052 cm/yr) based on the ^{210}Pb chronology of another sediment core from Lake Kanas (Feng and Ren 1990) is very close to the sedimentation rate calculated from our ^{14}C-based age model for the upper part of the core (0.05 cm/yr), which suggests that the residence time of terrestrial plants is relatively short and there is no obvious "old wood" effect (Huang et al. 2018). Therefore, the chronological framework based on these plant remains can be regarded as reliable.

The climatic and hydrological conditions of lakes during the Holocene were often variable, which led to spatial and temporal variations in the ^{14}C reservoir effect in different lakes. Although the combined application of ^{210}Pb, ^{137}Cs, and ^{14}C dating of the same surface sediment layer can be used to determine the reservoir age, this approach cannot be used to estimate the reservoir age in the earlier stages. Linear regression is widely used to estimate

the reservoir age (e.g., Fontes et al. 1996; Shen et al. 2005; Wu et al. 2010), and this method is applicable for stable environments and short-term depositional processes. In Lake Kanas, we simulated the age-depth model according to the ^{14}C ages of plant remains and TOC, and the R^2 values of the fitted curve are 0.9997 and 0.992, respectively (Figure 2a). The correlation between age and depth is significant. Accordingly, we calculated the radiocarbon reservoir age based on the simulated age model of plant remains and TOC, and we then simulated an idealized curve of the relationship of the radiocarbon reservoir age with depth (Figure 2b).

At the depths of 170 and 157 cm, the ^{14}C ages of terrestrial plant remains are slightly older than those dated with TOC, which could be caused by an "old wood" effect as mentioned above (Figure 2a). The "old wood" effect of the charcoal or charred wood could be caused by the longer residence time between the death of the plant and the deposition of the sediments, which usually produces a relatively old age (Payette et al. 2012). As the sediments of Lake Kanas are relatively fine-grained, there is a very low possibility of the downward penetration of younger organic matter (Figure 2c), which means that the TOC-based ^{14}C age could be reliable and that there was no radiocarbon reservoir effect. Deeper within the core the ages at the depths of 185–243 cm vary between 9500 and 10,060 ^{14}C BP, and several of the ^{14}C ages are slightly reversed during the Younger Dryas and earlier. The similar ^{14}C ages could be caused by a changing atmospheric ^{14}C concentration (Muscheler et al. 2008), a rapid sedimentation rate, and/or the downward penetration of younger organic material from the upper layer due to coarser sedimentary grain sizes as this time (see Huang et al. 2018).

The ^{14}C ages of the TOC gradually become older than those of the terrestrial plant remains and the reservoir age can be estimated for the upper ~156-cm interval of the core (Figure 2b). At the depth interval of 156–25 cm, the simulated ^{14}C ages of the terrestrial plant remains vary from ~8350 to ~540 BP, and the simulated ^{14}C ages of the TOC are much older. The reservoir ages increase from the lower part to the upper part of the sedimentary sequence, from nearly 0 to ~2800 yr. During the middle and late Holocene, the radiocarbon reservoir effect shows an increasing trend (Figure 2b).

Sources of TOC in the Sediments of Lake Kanas

Hydrological and climatic changes in northwest China could be the main factors responsible for the temporal changes in the ^{14}C reservoir ages of the lake sediments (Zhou et al. 2009, 2020). Studies of Lake Sugan and Lake Bosten showed that the reservoir effect was smaller during humid intervals, and significantly larger during dry intervals. Hypersaline lake water may undergo ^{14}C exchange between the water and the atmosphere, leading to a smaller proportion of the ^{14}C in the water than in air during the same interval, resulting in an increase in the radiocarbon reservoir effect (Zhou et al. 2009, 2020).

Lake Kanas is a freshwater lake fed mainly by a river in the north and previous studies found that carbonate is absent from the sediments (Wu et al. 2014); therefore, the amount of "dead" inorganic carbon dissolved in the water should be very low and can be ignored. Additionally, Lake Kanas is relatively deep and the bathymetry is steeply sloping due to erosion by earlier glaciations, with very low biological productivity and almost no aquatic plants (Feng and Ren 1990). Our field observations and investigations showed that meltwater during the spring and heavy rainfall in the summer often carry soil from the mountain slopes into the lake, and the floodwater has a dark peaty color. Therefore, the TOC in Lake Kanas is much more likely to
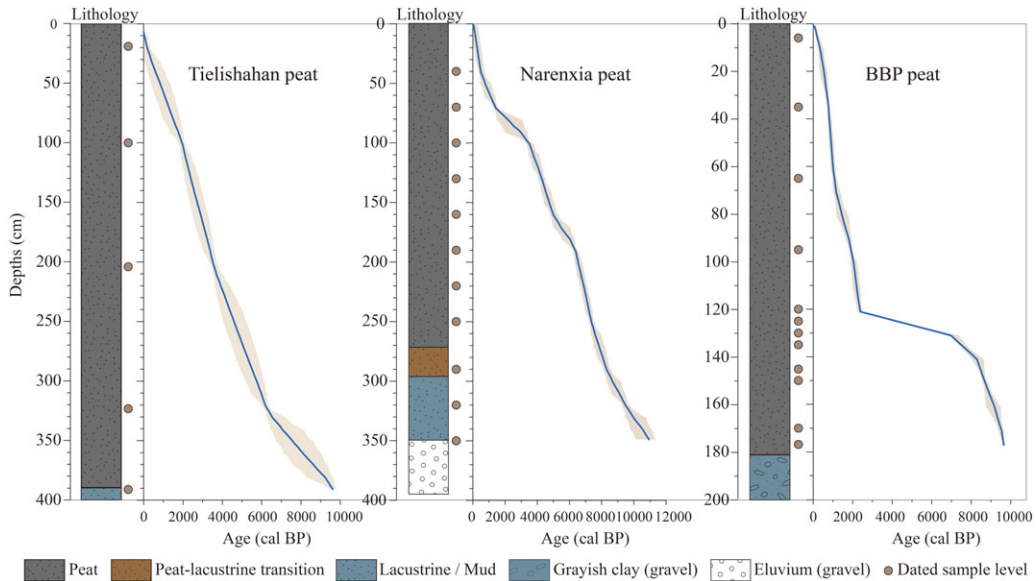
Figure 3   Stratigraphy and Bacon age-depth models for peat deposits in the vicinity of Lake Kanas: Tielishahan peatland (Zhang et al. 2016); Narenxia peatland (Feng et al. 2017); Big Black peatland (BBP) (Xu et al. 2019).

originate within the watershed than be produced within the water column. Moreover, the $\delta^{13}C$ of the 7 ^{14}C-dated sediment samples varied between –25.7‰ and –21.5‰, which is very close to the values of the plant remains (Table 1), in both cases indicating that the source of the organic material is terrestrial C_3 trees and shrubs ($\delta^{13}C$: –31 to –23‰) (Meyers and Teranes 2002). The $\delta^{15}N$ values of the 7 sediment samples varied between 3.8‰ and 7.1‰, which is typical of terrestrial plants ($\delta^{15}N$: ~4.5–10.3‰), rather than aquatic plants ($\delta^{15}N$: ~12.8‰) (Talbot and Johannessen 1992). Hence, we infer that the TOC in the sediments of Lake Kanas is of allochthonous rather than autochthonous origin. Additionally, it is worth noting that the C/N ratios of the sediments varied between 9.0 and 14.1, which indicates a mixture of aquatic and terrestrial plant materials (Cook et al. 2012). However, we suspect that the extremely low N content (~0.1%) may lead to large uncertainties in the C/N ratios, which requires further study.

Peat accumulation was widespread in the study area during the Holocene. We reconstructed the relationship between the calendar age and depth in three previously reported peat cores (Zhang et al. 2016; Feng et al. 2017; Xu et al. 2019), using the Bacon program with all of the default settings (Figure 3). The Big Black peatland (BBP), ~11 km to the east of Lake Kanas, begun to develop from ~9500 cal BP (Figure 3, Xu et al. 2019). Similarly, the ages of the Tielishahan and Narenxia peatlands, ~8 km to the west of Lake Kanas, show that the peats began to accumulate from ~9000 cal BP, and ~9600 cal BP, respectively (Figure 3; Zhang et al. 2016; Feng et al. 2017). Due to the effects of glaciation, there was minimal soil development in the region during the Last Glacial period, and soils developed mainly on the mountain slopes around Lake Kanas during ~9600–9000 cal BP. Lake Kanas lies in a steep gorge and the soil on both sides of the mountain slopes is easily eroded by runoff. Therefore, we infer that organic material from watershed soils and peats is the dominant source of the organic material in the lake sediments.
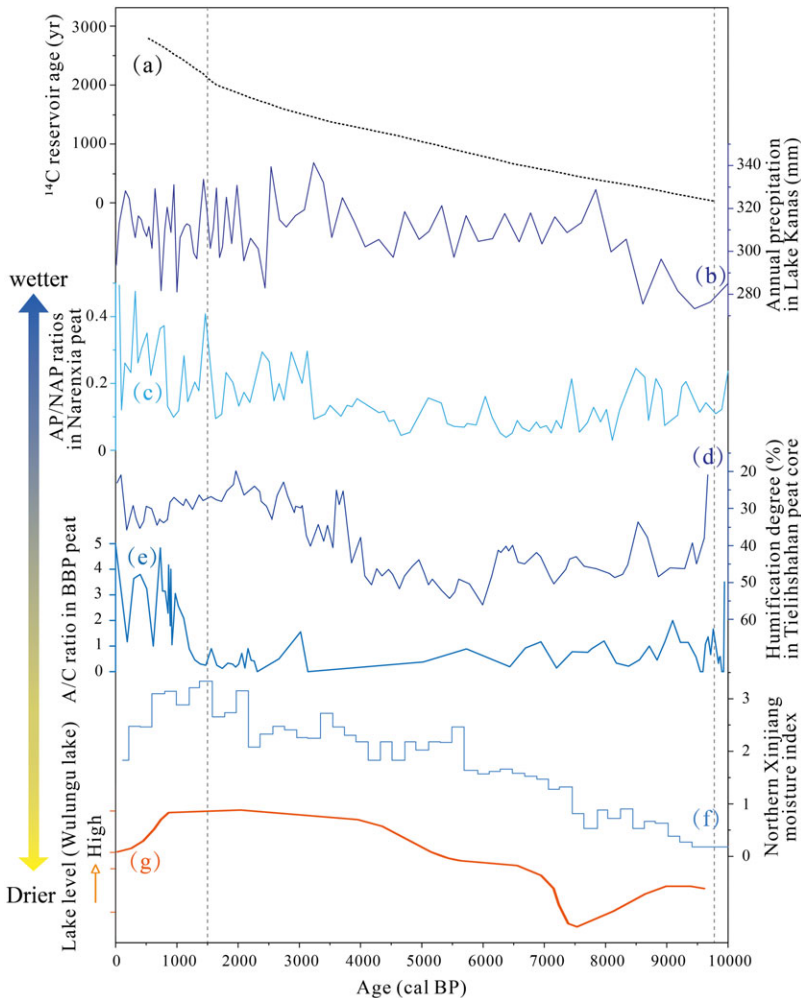
Figure 4   Temporal variation of the radiocarbon reservoir age at Lake Kanas compared with various regional paleoclimatic records. (a) Radiocarbon reservoir age at Lake Kanas; (b) quantitative annual precipitation reconstructed for Lake Kanas (Huang et al. 2018); (c) arboreal pollen/non-arboreal pollen (AP/NAP) ratio from the Narenxia peatland (Feng et al. 2017); (d) humification record from the Tielishahan peatland (Zhang et al. 2016); (e) *Artemisia*/Chenopodiaceae (A/C) pollen ratio from the Big Black peatland (BBP) (Xu et al. 2019); (f) moisture evolution of the northern Xinjiang region (Wang and Feng 2013); (g) lake level record of Lake Wulungu (Liu et al. 2008).

Soil Erosion Caused by High Humidity/Precipitation Was Responsible for the Radiocarbon Reservoir Effect at Lake Kanas during the Mid-to-Late Holocene

The chronological framework of lake sedimentation was reconstructed based on the ^{14}C dates of plant remains, implemented with the Bacon program, using the Intcal20 calibration. A radiocarbon reservoir effect was evident and the reservoir age gradually increased after ∼9700 cal BP (Figure 4a). As discussed above, soils and peats on the mountain slopes were the major sources of organic material in the sediments of Lake Kanas during the Holocene, and this eroded organic material would have had varying ages. Thus, we suggest that the
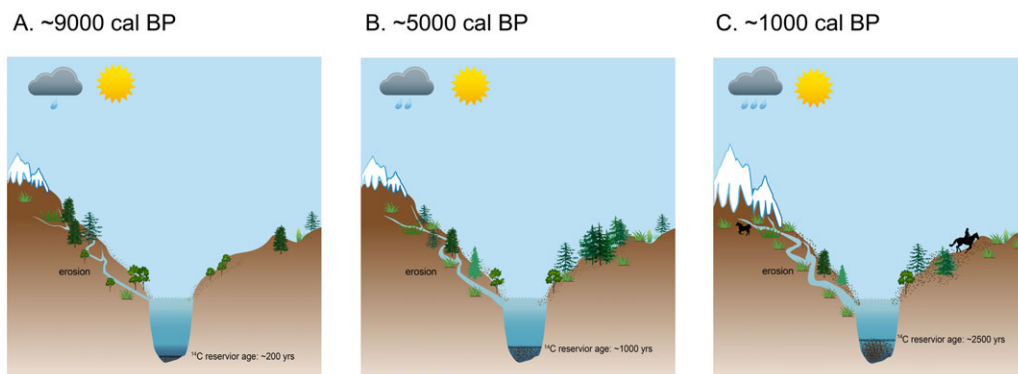
Figure 5   Schematic diagram illustrating the origin of the trend of increasing radiocarbon reservoir age at Lake Kanas.

continuous supply of progressively older organic matter from eroding soils/peats from ~9700 cal BP to the present-day was responsible for the increasing ^{14}C reservoir age of the sedimentary TOC in Lake Kanas.

The intensity of soil erosion in watersheds is mainly controlled by flood frequency and intensity, soil availability, vegetation conditions, and human activities (He et al. 2006; Zheng 2006; Huang et al. 2021b; Chen et al. 2022). A pollen-based quantitative annual precipitation reconstruction from Lake Kanas indicated the occurrence of high humidity/ precipitation during the mid-to late Holocene (Figure 4b; Huang et al. 2018), which is supported by many other regional paleoclimatic records (Figure 4f, g; Liu et al. 2008; Sun et al. 2013; Chen F et al. 2016; Chen H et al. 2019). The pollen-based precipitation reconstruction for Lake Kanas indicates slightly higher precipitation during the mid-Holocene compared to the late Holocene, which appears to be inconsistent with our inference of increasing soil/peat erosion during the late Holocene caused by higher precipitation. However, annual precipitation reconstructed by pollen data may be biased to precipitation falling during the vegetation growing and it may not reflect the contribution of winter snowfall. Winter snowfall contributes almost half of the annual precipitation in the study region, and while snow meltwater in spring has a limited influence on vegetation growth it has a large impact on soil erosion, as meltwater floods are frequent in the region. During the late Holocene, several glacier advances occurred in the Altai Mountains (Agatova et al. 2012, 2021), which further demonstrates an increase in winter snowfall in the mountains around Lake Kanas. Various geochemical indexes from the Tielishahan, Narenxia, and Big Black peatlands, located around Lake Kanas (Figure 1), also indicate a wetting trend in the late Holocene (Figure 4c–e; Zhang et al. 2016; Feng et al. 2017; Xu et al. 2019).

Huang et al. (2018) have provided a detailed discussion of the regional vegetation dynamics during the Holocene. Three major stages in the vegetation evolution can be defined: the development of forest vegetation during the early Holocene; maximum forest coverage during the mid-Holocene; and the varying development of forest steppe during the late Holocene. However, climatically-controlled vegetation dynamics arguably were not the principal control on the intensity of soil erosion. Over the past ~1500 years, human activity may have resulted in forest clearance and the reduction of the regional tree cover (Huang

et al. 2018). Forest clearance for pastoralism, especially, would have caused an increase in the rate of soil erosion.

A schematic diagram illustrating the temporal pattern of soil erosion and its relationship with the old carbon effect is shown in Figure 5. During the early Holocene, the low tree coverage and limited accumulation of soil carbon resulted in the very limited supply of soil-derived old carbon to the lake sediments. However, the progressively wetting climate during the mid-to late Holocene promoted the increased accumulation of soil organic matter and peat, as well as causing an increase in soil erosion and thus the ^{14}C reservoir age.

CONCLUSION

Discrepancies between the ^{14}C ages of the TOC and terrestrial plant remains in the Holocene sediments of Lake Kanas reveal temporal variations in the radiocarbon reservoir effect. The radiocarbon reservoir effect increased progressively from 0 yr at ~9700 cal BP to ~2800 ^{14}C yr at ~530 cal BP. The erosion of soils and peat deposits in the mountains around Lake Kanas resulted in the supply of old organic carbon to the lake sediments. Additionally, we suggest that the supply of eroded organic material from different soil and peat depths resulted in the observed variations of the reservoir effect evident in the radiocarbon ages of the sedimentary TOC in Lake Kanas. Increased precipitation in the region during the mid-to late Holocene was responsible for soil organic matter and peat accumulation and their subsequent erosion, causing an increase in the age of the organic matter entering the lake, which in turn increased the radiocarbon reservoir effect. Therefore, climate change, especially the occurrence of snow meltwater–derived flooding, was the principal factor responsible for the observed change in the radiocarbon reservoir effect at Lake Kanas. During the past ~1500 years, human activity may also have caused a further increase in soil erosion. Our results are of broad significance for the radiocarbon dating of the TOC of lake sediments which lack plant macrofossils, and they provide a foundation for past and future studies of lake sediment–based Holocene climate change in the region.

ACKNOWLEDGMENTS

DECLARATION OF COMPETING INTEREST

The authors declare that they have no conflict of interest.

REFERENCES

Agatova AR, Nazarov AN, Nepop RK, Rodnight H. 2012. Holocene glacier fluctuations and climate changes in the southeastern part of the Russian Altai (South Siberia) based on a radiocarbon chronology. Quaternary Science Reviews 43:74–93.

Agatova A, Nepop R, Nazarov A, Ovchinnikov I, Moska P. 2021. Climatically driven Holocene glacier advances in the Russian Altai based on radiocarbon and OSL dating and tree ring analysis. Climate 9(11):162.

Aizen EM, Aizen VB, Melack JM, Nakamura T, Ohta T. 2001. Precipitation and atmospheric circulation patterns at mid-latitudes of Asia. International Journal of Climatology: A Journal of the Royal Meteorological Society 21(5):535–556.

An F, Lai Z, Liu X, Wang Y, Chang Q, Lu B, Yang X. 2018. Luminescence chronology and radiocarbon reservoir age determination of lacustrine sediments from the Heihai Lake, NE

Qinghai-Tibetan Plateau and its paleoclimate implications. Journal of Earth Science 29(3):695–706.

Andree M, Oeschger H, Siegenthaler U, Riesen T, Moell M, Ammann B, Tobolski K. 1986. ^{14}C dating of plant macrofossils in lake sediment. Radiocarbon 28(2A):411–416.

Björck S, Wohlfarth B. 2001. ^{14}C chronostratigraphic techniques in paleolimnology. In: Last W, Smol JP, editors. Tracking environmental change using lake sediments. basin analysis, coring and chronological techniques, 1. Netherlands: Kluwer Academic Publishers. p. 205–245.

Blaauw M, Christen JA. 2011. Flexible paleoclimate age-depth models using an autoregressive gamma process. Bayesian Analysis 6(3):457–474.

Blaauw M, van Geel B, Kristen I, Plessen B, Lyaruu A, Engstrom DR, van der Plicht J. Verschuren D. 2011. High-resolution ^{14}C dating of a 25,000-year lake-sediment record from equatorial East Africa. Quaternary Science Reviews 30(21–22):3043–3059.

Bonk A, Tylmann W, Goslar T, Wacnik A, Grosjean, M. 2015. Comparing varve counting and ^{14}C-AMS chronologies in the sediments of Lake Żabińskie, Northeastern Poland: implications for accurate ^{14}C dating of lake sediments. Geochronometria 42(1):159–171.

Bureau of National Cultural Relics. 2012. Atlas of Chinese cultural relics—fascicule of Xinjiang Uygur autonomous region. Beijing: China Cartographic Publishing House Press. In Chinese.

Chen F, Jia J, Chen J, Li G, Zhang X, Xie H, Xia D, Huang W, An C. 2016. A persistent Holocene wetting trend in arid central Asia, with wettest conditions in the late Holocene, revealed by multi-proxy analyses of loess-paleosol sequences in Xinjiang, China. Quaternary Science Reviews 146:134–146.

Chen F, Chen J, Huang W, Chen S, Huang X, Jin L, Jia J, Zhang X, An C, Zhang J, Zhao Y, Yu Z, Zhang R, Liu J, Zhou A, Feng S. 2019. Westerlies Asia and monsoonal Asia: Spatiotemporal differences in climate change and possible mechanisms on decadal to sub-orbital timescales. Earth-Science Reviews 192: 337–354.

Chen H, Zhu L, Ju J, Wang J, Ma Q. 2019. Temporal variability of ^{14}C reservoir effects and sedimentological chronology analysis in lake sediments from Chibuzhang Co, North Tibet (China). Quaternary Geochronology 52:88–102.

Chen X, Huang X, Wu D, Chen J, Zhang J, Zhou A, Dodson J, Zawadzki A, Jacobsen G, Yu J, Wu Q, Chen F. 2022. Late Holocene land use evolution and vegetation response to climate change in the watershed of Xingyun Lake, SW China. Catena 211:105973.

Cook CG, Leng MJ, Jones RT, Langdon PG, Zhang E. 2012. Lake ecosystem dynamics and

links to climate change inferred from a stable isotope and organic palaeorecord from a mountain lake in southwestern China (ca. 22.6–10.5 cal ka BP). Quaternary Research 77(1):132–137.

Druffel EM, Suess HE. 1983. On the radiocarbon record in banded corals: exchange parameters and net transport of $^{14}CO_2$ between atmosphere and surface ocean. Journal of Geophysical Research: Oceans 88(C2):1271–1280.

Fan Q, Ma H, Ma Z, Wei H, Han F. 2014. An assessment and comparison of ^{230}Th and AMS ^{14}C ages for lacustrine sediments from Qarhan Salt Lake area in arid western China. Environmental Earth Sciences 71(3):1227–1237.

Feng Z, Sun A, Abdusalih N, Ran M, Kurban A, Lan B, Zhang D, Yang Y. 2017. Vegetation changes and associated climatic changes in the southern Altai Mountains within China during the Holocene. The Holocene 27(5):683–693.

Feng M, Ren M. 1990. Scientific investigation on Kanas Lake in Xinjiang. Beijing: Science Press. In Chinese.

Fontes JC, Gasse F, Gibert E. 1996. Holocene environmental changes in Lake Bangong basin (Western Tibet). Part 1: Chronology and stable isotopes of carbonates of a Holocene lacustrine core. Palaeogeography, Palaeoclimatology, Palaeoecology 120(1–2):25–47.

Frueh WT. 2012. Sediment reservoir dynamics on steep land valley floors: Influence of network structure and effects of inherited ages [Master's dissertation].Oregon State University.

Hall BL, Henderson GM. 2001. Use of uranium–thorium dating to determine past ^{14}C reservoir effects in lakes: examples from Antarctica. Earth and Planetary Science Letters 193(3–4):565–577.

He X, Zhou J, Zhang X, Tang K. 2006. Soil erosion response to climatic change and human activity during the Quaternary on the Loess Plateau, China. Regional Environmental Change 6(1):62–70.

Hou G, D'Andrea WJ, Liu Z. 2012. The influence of ^{14}C reservoir age on interpretation of paleolimnological records from the Tibetan Plateau. Quaternary Science Reviews 48:67–79.

Huang X, Peng W, Rudaya N, Grimm EC, Chen X, Cao X, Zhang J, Pan X, Liu S, Chen C, Chen F. 2018. Holocene vegetation and climate dynamics in the Altai Mountains and surrounding areas. Geophysical Research Letters 45(13):6628–6636.

Huang X, Ren X, Chen X, Zhang J, Zhang X, Shen Z, Hu Y, Chen, F. 2021b. Anthropogenic mountain forest degradation and soil erosion recorded in the sediments of Mayinghai Lake in northern China. Catena 207:105597.

Huang X, Xiang L, Lei G, Sun M, Qiu M, Storozum M, Huang C, Munkhbayar C, Demberel O, Zhang J, Zhang J, Chen X, Chen J, Chen F. 2021a. Sedimentary *Pediastrum* record of

middle–late Holocene temperature change and its impacts on early human culture in the desert-oasis area of northwestern China. Quaternary Science Reviews 265:107054. doi: 10.1016/j.quascirev.2021.107054.

Huang XZ, Chen FH, Fan YX, Yang ML. 2009. Dry late-glacial and early Holocene climate in arid central Asia indicated by lithological and palynological evidence from Bosten Lake, China. Quaternary International 194(1–2):19–27.

Shen J, Liu X, Wang S, Matsumoto, R. 2005. Palaeoclimatic changes in the Qinghai Lake area during the last 18,000 years. Quaternary International 136(1):131–140.

Kwiecien O, Arz HW, Lamy F, Wulf S, Bahr A, Röhl U, Haug GH. 2008. Estimated reservoir ages of the Black Sea since the last glacial. Radiocarbon 50(1):99–118.

Lan B, Zhang D, Yang Y. 2018. Lacustrine sediment chronology defined by ^{137}Cs, ^{210}Pb and ^{14}C and the hydrological evolution of Lake Ailike during 1901–2013, northern Xinjiang, China. Catena 161 :104–112.

Li Y, Qiang M, Jin Y, Liu L, Zhou A, Zhang J. 2018. Influence of aquatic plant photosynthesis on the reservoir effect of Genggahai Lake, northeastern Qinghai-Tibetan Plateau. Radiocarbon 60(2):561–569.

Lin X, Rioual P, Peng W, Yang H, Huang X. 2018. Impact of recent climate change on Lake Kanas, Altai Mountains (NW China) inferred from diatom and geochemical evidence. Journal of paleolimnology 59(4):461–477.

Liu CH, You GX, Pu JC. 1982. Glacier Inventory of China II: Altay Mountains. Lanzhou Institute of Glaciology and Cryopedology, Academia Sinica, Lanzhou. p. 1–87. In Chinese.

Liu X, Herzschuh U, Shen J, Jiang Q, Xiao X. 2008. Holocene environmental and climatic changes inferred from Wulungu Lake in northern Xinjiang, China. Quaternary Research 70(3):412–425.

Meyers PA, Teranes JL. 2002. Sediment organic matter—tracking environmental change using lake sediments. Dordrecht: Springer. p. 239–269.

Mischke S, Weynell M, Zhang C, Wiechert U. 2013. Spatial variability of ^{14}C reservoir effects in Tibetan Plateau lakes. Quaternary International 313:147–155.

Muscheler R, Kromer B, Björck S, Svensson A, Friedrich M, Kaiser KF, Southon J. 2008. Tree rings and ice cores reveal ^{14}C calibration uncertainties during the Younger Dryas. Nature Geoscience 1(4):263–267.

Olsson IU. 2009. Radiocarbon dating history: early days, questions, and problems met. Radiocarbon 51(1):1–43.

Payette S, Delwaide A, Schaffhauser A, Magnan G. 2012. Calculating long-term fire frequency at the stand scale from charcoal data. Ecosphere 3(7):1–16.

Ramsey CB. 2009. Bayesian analysis of radiocarbon dates. Radiocarbon 51(1):337–360.

Rao Z, Shi F, Li Y, Huang C, Zhang X, Yang W, Liu L, Zhang X, Wu Y. 2020. Long-term winter/summer warming trends during the Holocene revealed by α-cellulose δ^{18}O/δ^{13}C records from an alpine peat core from central Asia. Quaternary Science Reviews 232:106217.

Reimer PJ, Austin WE, Bard E, Bayliss A, Blackwell PG, Ramsey CB, Butzin M, Cheng H, Edwards RL, Friedrich M, Grootes PM, Guilderson TP, Hajdas I, Heaton TJ, Hogg AG, Hughen KA, Kromer B, Manning SW, Muscheler R, Palmer JG, Pearson C, van der Plicht J, Reimer RW, Richards DA, Scott EM, Southon JR, Turney CSM, Wacker L, Adolphi F, Büntgen U, Capano M, Fahrni SM, Fogtmann-Schulz A, Friedrich R, Köhler P, Kudsk S, Miyake F, Olsen J, Frederick R, Sakamoto M, Sookdeo A Talamo S. 2020. The IntCal20 Northern Hemisphere radiocarbon age calibration curve (0–55 cal kBP). Radiocarbon 62(4):725–757.

Schroeter N, Mingram J, Kalanke J, Lauterbach S, Tjallingii R, Schwab VF, Gleixner G. 2021. The reservoir age effect varies with the mobilization of pre-aged organic carbon in a high-altitude Central Asian catchment. Frontiers in Earth Science 9:532.

Sun A, Feng Z, Ran M, Zhang C. 2013. Pollen-recorded bioclimatic variations of the last ~22,600 years retrieved from Achit Nuur core in the western Mongolian Plateau. Quaternary International 311:36–43.

Talbot MR, Johannessen T. 1992. A high resolution palaeoclimatic record for the last 27,500 years in tropical West Africa from the carbon and nitrogen isotopic composition of lacustrine organic matter. Earth and Planetary Science Letters 110(1–4):23–37.

Tang Y. 2014. Holocene environmental changes inferred from GDGTs from peatlands in the Altai Mountains, Xinjiang of China [master's thesis]. Lanzhou University of China. In Chinese.

Tlan J, Brown TA, Hul FS. 2005. Comparison of varve and ^{14}C chronologies from Steel Lake, Minnesota, USA. The Holocene 15(4):510–517.

Wang W, Feng Z. 2013. Holocene moisture evolution across the Mongolian Plateau and its surrounding areas: A synthesis of climatic records. Earth-Science Reviews 122: 38–57.

Wang W, Zhang D. 2019. Holocene vegetation evolution and climatic dynamics inferred from an ombrotrophic peat sequence in the southern Altai Mountains within China. Global and Planetary Change 179:10–22.

Wang YH, Huang XZ, Peng W, Zhou GP, Zhang J, Du X. 2017. Temperature variations over the past 600 years documented by a δ^{13}C record from terrestrial plant remains from Kanas Lake,

Altai Mountains, Northwestern China. Chinese Science Bulletin 62(24):2829–2839. In Chinese with English abstract.

Watanabe T, Matsunaka T, Nakamura T, Nishimura M, Sakai T, Lin X, Horiuchi K, Nara FW, Kakegawa T, Zhu L. 2010. [14]C dating of Holocene soils from an island in Lake Pumoyum Co (southeastern Tibetan plateau). Radiocarbon 52(3):1443–1448.

Wilkins D, De Deckker P, Fifield LK, Gouramanis C, Olley J. 2012. Comparative optical and radiocarbon dating of laminated Holocene sediments in two maar lakes: Lake Keilambete and Lake Gnotuk, south-western Victoria, Australia. Quaternary Geochronology 9:3–15.

Wu J, Liu W, Zeng H, Ma L, Bai R. 2014. Water quantity and quality of six lakes in the arid Xinjiang region, NW China. Environmental Processes 1(2):115–125.

Wu Y, Li S, Lücke A, Wünnemann B, Zhou L, Reimer P, Wang S. 2010. Lacustrine radiocarbon reservoir ages in Co Ngoin and Zigê Tangco, central Tibetan plateau. Quaternary International 212(1):21–25.

Xinjiang Comprehensive Survey Team, C. A. o. S., & Institute of Botany, C. A. o. S. 1978. Xinjiang vegetation and its utilization. Beijing: Science Press. In Chinese.

Xu D, Lu H, Jin C, Gu Z, Zuo X, Dong Y, Wang C, Wang L, Li H, Yu Y, Jin Y, Wu N. 2021. Application of multiple dating techniques to the Holocene sediments of Angrenjin Co in the southern Tibetan Plateau. Quaternary Geochronology 62: 101148. doi: 10.1016/j. quageo.2020.101148.

Xu H, Lan J, Zhang G, Zhou X. 2019. Arid central Asia saw mid-Holocene drought. Geology 47(3):255–258.

Xu X, Yang J, Dong G, Wang L, Miller L. 2009. OSL dating of glacier extent during the Last Glacial and the Kanas Lake basin formation in Kanas River valley, Altai Mountains, China. Geomorphology 112(3-4):306–317.

Zhang D, Feng Z, Yang Y, Lan B, Ran M, Mu G. 2018a. Peat δ^{13}Ccelluose-recorded wetting trend during the past 8000 years in the southern Altai Mountains, northern Xinjiang, NW China. Journal of Asian Earth Sciences 156:174–179.

Zhang D, Yang Y, Lan B. 2018b. Climate variability in the northern and southern Altai Mountains during the past 50 years. Scientific Reports 8(1):1–11.

Zhang Q, Liu X, Li H. 2021. Impact of hydrological conditions on the radiocarbon reservoir effect in lake sediment ^{14}C dating: the case of Kusai Lake on the northern Qinghai-Tibet Plateau. Quaternary Geochronology 62:101149. doi: 10. 1016/j.quageo.2020.101149.

Zhang T, Elias SA. 2019. Holocene palaeoenvironmental reconstruction based on fossil beetle faunas from the Southern Altai region, north-west China. Journal of Quaternary Science 34(8):593–602.

Zhang Y, Meyers PA, Liu X, Wang G, Ma X, Li X, Yuan Y, Wen B. 2016. Holocene climate changes in the central Asia mountain region inferred from a peat sequence from the Altai Mountains, Xinjiang, northwestern China. Quaternary Science Reviews 152:19–30.

Zheng F. 2006. Effect of vegetation changes on soil erosion on the Loess Plateau. Pedosphere 16(4):420–427.

Zhou A, He Y, Wu D, Zhang X, Zhang C, Liu Z, Yu J. 2015. Changes in the radiocarbon reservoir age in Lake Xingyun, Southwestern China during the Holocene. PLoS One 10(3): e0121532. doi: 10.1371/journal.pone.0121532.

Zhou A, Chen F, Wang Z, Yang M, Qiang M, Zhang J. 2009. Temporal change of radiocarbon reservoir effect in Sugan Lake, northwest China during the late Holocene. Radiocarbon 51(2):529–535.

Zhou K, Xu H, Lan J, Yan D, Sheng E, Yu K, Song Y, Zhang J, Fu P, Xu S. 2020. Variable late Holocene ^{14}C reservoir ages in lake Bosten, Northwestern China. Frontiers in Earth Science 7:328. doi: 10.3389/feart.2019.00328.

Zhou W, Cheng P, Jull AT, Lu X, An Z, Wang H, Zhu Y, Wu Z. 2014. [14]C chronostratigraphy for Qinghai Lake in China. Radiocarbon 56(1):143–155.

Zhou W, Chui Y, Yang L, Cheng P, Chen N, Ming G, Hu Y, Li W, Lu X. 2021. [14]C Geochronology and Radiocarbon reservoir effect of reviewed lakes study in China. Radiocarbon: 1–12. doi: 10. 1017/RDC.2021.92.